# Extreme ultraviolet radiation of transient plasma in fast conical discharge

P. S. Antsiferov,[1,2,*] L. A. Dorokhin,[1] and K. N. Koshelev[1]
[1]*Institute of Spectroscopy of Russian Academy of Sciences, Fizicheskaya strasse 5, 108840 Troitsk, Moscow, Russia*
[2]*Moscow Institute of Physics and Technology, Institutsky line 9, 141700 Dolgoprudny, Russia*

(Received 7 June 2019; published 22 August 2019)

The article presents the results of the detailed experimental study of fast conical discharge with Ar as a working gas. The discharge produces a compact transient plasma which emits extreme ultraviolet (EUV) radiation with wavelength 10.8 nm. The intensity of this spectral line is an order of magnitude larger than the rest of the radiation in EUV band. Space resolved EUV spectra allowed us to get the estimation of the effective size of the radiation source (less than 0.5 mm). Time resolved spectra (frame time 20 ns) show that a 10.8-nm spectral line is emitted during 50–60 ns. Charge exchange of Ar IX ions with excited atoms of Ar I in the result of interaction of hot compact plasma in the cumulation point of conical shockwave and cold working gas is considered as the main phenomenon, responsible for the emission of the detected radiation.

DOI: 10.1103/PhysRevE.100.023204

## I. INTRODUCTION

A practical problem of the development of the sources of extreme ultraviolet (EUV) radiation motivates the investigation of hot dense plasma of electrical discharges. This method of plasma generation is simple and comparatively cheap, but the underlying physical phenomena are intricate and difficult for the detailed theoretical modeling. So the experimental study is an important source of the information about hot dense plasma of electrical discharges. The present work deals with fast discharges, which had appeared the first time as method of generation of stimulated emission in soft x-ray spectral region (capillary discharge) [1]. Fast discharge is an electrical discharge through a gas filled cavity ($P \cong 100$ Pa) with a current rise rate about $10^{12}$ A/s and the value of maximal current of several tens of kA. The general features of capillary discharge were analyzed in [2]. The central phenomenon is the concentration of the discharge current near the inner surface of the ceramic capillary pipe due to skin effect and generation of the convergent cylindrical shock wave. Here a high current rise rate is the necessary condition for the skin effect. A fast collapse of shock wave results in appearance of hot plasma column with aspect ratio up to 1:1000, where the population inversion on the $3s-3p$ transition in Ne-like Ar exists during several nanoseconds.

The spatial structure of the convergent shock wave in fast discharge is defined by the inner profile of the discharge cavity. This makes it possible to get hot plasma of different shapes. So, the usage of a discharge cavity with the inner surface close to spherical (spherical belt) allows us to get spherical plasma [3]. In the case of a discharge cavity with conical inner surface [see Fig. 1(a)] it seems to be possible to get the collapse point, which moves effectively along the discharge axis due to "zippering" of the convergent conical shock wave. The previous work [4] confirmed this scenario. It was also reported in [4], that such discharge produces a strong emission line at 10.8 nm. The present work is devoted to detailed experimental study of the radiation of fast conical discharge with the usage of spatially resolved EUV spectra. The analysis of the possible mechanism of the appearance of this radiation is also presented.

## II. PINHOLE CAMERA MEASUREMENTS

The discharge circuit was described in [5] (inductive storage with semiconductor opening switch). It was able to create the current in the load with rise rate about $10^{12}$ A/s and maximal value 25−30 kA. The discharge cavity was produced as an alumina unit with 12 mm length, front and rear diameters of conical cavity are 7 and 3 mm respectively. The cavity was filled with Ar at 80 Pa, which is around optimal for EUV emission. An off-axis pinhole camera [see Fig. 1(b)] was able to give information about the axial motion of the discharge plasma. A microchannel plate (MCP) detector with time gate 5 ns was used for the image detection. The time evolution of the discharge plasma structure is demonstrated in Fig. 2. The times of frames are given with respect to the start of the discharge current. Ring features in the frames 15–20 and 35–40 ns reflect the position of the front of the convergent conical shock wave in the rear aperture of conical discharge cavity. Visible motion of the collapse point is not a real plasma motion, it is a result of the "zippering" of convergent conical shock wave. The main difference between conical discharge and capillary discharge [1] is that the collapse of cylindrical shock wave takes place simultaneously on the discharge axis, and in the case of conical discharge at a certain moment it takes place in one point on the axis of discharge. The conical shock wave starts to collapse at 50 ns after the beginning of the discharge current, and the motion of the collapse point can be traced up to 140–150 ns. That gives the estimation of the velocity of effective axial motion of hot plasma as $10^7$ cm/s.

*Corresponding author: Ants@isan.troitsk.ru

 

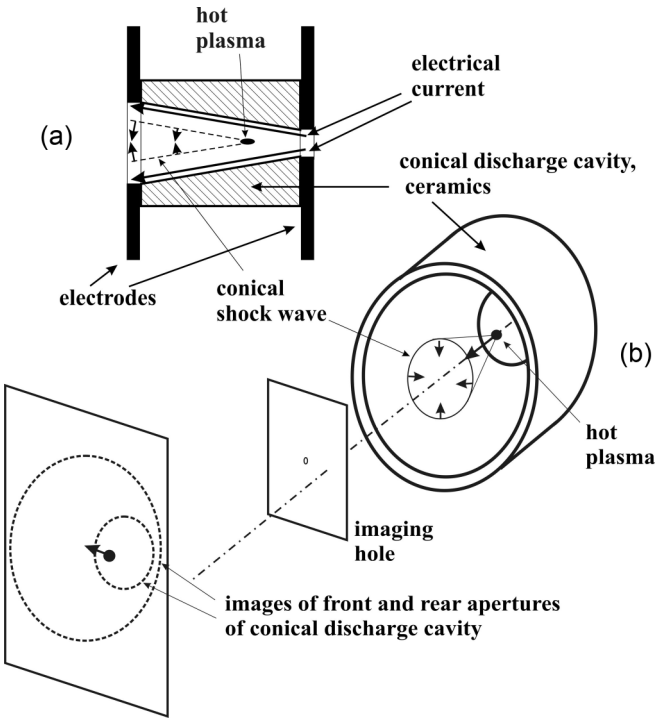


FIG. 1. (a) The scheme of conical discharge. (b) Off-axis pinhole camera arrangement.

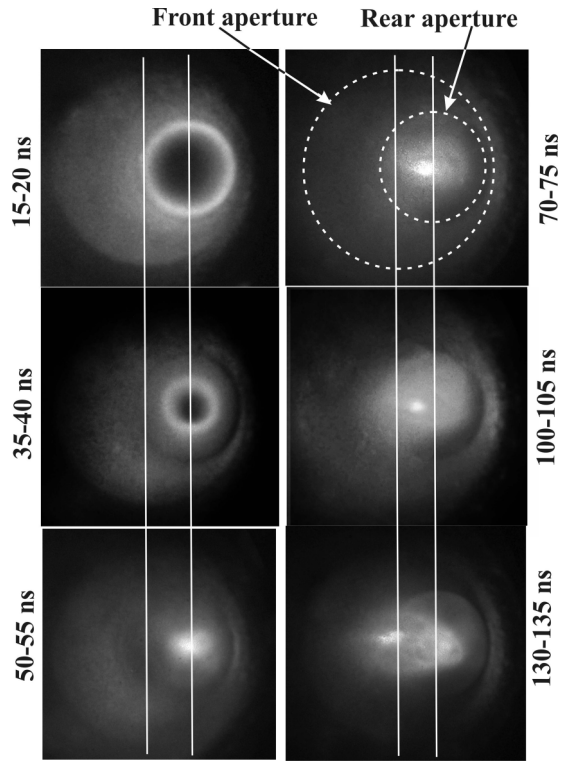


FIG. 2. Time evolution of discharge plasma. A set of pinhole camera images; times of frames are given with respect to the beginning of the discharge current. Vertical white lines give the positions of the images of centers of front and rear apertures of conical discharge cavity.

## III. SPATIALLY AND TEMPORALLY RESOLVED EUV SPECTRA

The EUV spectra were obtained by means of a grazing incidence spectrometer with spherical grating. The shift of the spectral slit inside the Rowland circle allows us to get the focusing of the spectrum normally to the line of sight (quasiflat field) [6]. The last circumstance is important for the use of a MCP detector for the registration of the spectra (time gating is 20 ns apart from 35 ns in the work [4]). The usage of the spherical grating with radius of curvature $R = 1$ m and groove density 1200 gr/mm (entrance slit is 10 μm) allowed us to get two times increase of the spectral resolution in comparison with [4]. The entrance grazing angle was 4°. According to [6] the distance slit grating was 33 mm and the distance grating spectrum was 320 mm. The total scheme of the spectral measurements, including a horizontal slit for the spatial resolution (0.4 mm), is shown in Fig. 3. The geometrical magnification of the radiation source in the direction of spatial resolution was 1:8.

An example of the detected spectra is given in Fig. 4. Strong emission at 10.8 nm, which was reported in [4], can be seen in the first and the second orders of diffraction grating. The visible size of its source is about 0.5 mm. Taking into account the input of the width in the horizontal slit, which was 0.4 mm, it is unambiguously connected with compact hot plasma, moving along the axis of the discharge (see Fig. 2). The correspondent spectral profiles are given in Fig. 5. Spectrum (a) corresponds to the start of the conical shock wave collapse (the timing is 40–60 ns from the start of the discharge current), spectrum (b) refers to the later moment (70–90 ns). The most prominent feature of spectrum (a) is the 10.8-nm spectral line. Its intensity exceeds by about an order of magnitude the total intensity in the rest of the EUV spectral range under consideration. The other spectral lines were identified according to [7]. Together with 10.8-nm line, the spectrum (a) contains also the lines of transitions $2s$-$3p$, $2p$-$3d$ and $2p$-$3s$ in OVI (ionization potential $I_{\mathrm{OVI}} = 123.1$ eV [7]), transitions $3s$-$4p$, $3p$-$4d$ in Ar VIII ($I_{\mathrm{Ar\ VIII}} = 143.4$ eV) and inner transitions $2s$-$2p$ in Ar X ($I_{\mathrm{Ar\ X}} = 478.7$ eV). Spectrum (b) contains the lines of Al and F ions, which were eroded from the inner wall and from the insulation of the discharge cavity. Figure 4(b) shows that these lines are emitted by the source of larger size than the 10.8-nm line source. It corresponds to a diffuse feature around compact plasma in Fig. 2 (70–75-nm and 100–105-nm frames). The intensity of 10.8 nm goes to 0 after 100 ns, although the compact plasma can be traced up to 130 ns after the beginning of the discharge (see Fig. 2).

The efficiency of our spectrometer in the spectral region of the resonance transitions in Ar IX and Ar X (3–5 nm) is small. The blaze angle of the grating 2.5° makes the maximum of the diffracted radiation at the wavelength about 20 nm. Nevertheless the spectra in this spectral range were obtained by the increase of the sensitivity of MCP through the increase of the gating voltage (the rest of the spectrum was oversaturated). The example of the spectrum is given in Fig. 6. Its general view does not change considerably in time range 50–100 ns from the beginning of the discharge, but the intensity goes down and after 100 ns it can't be seen any more. The presence

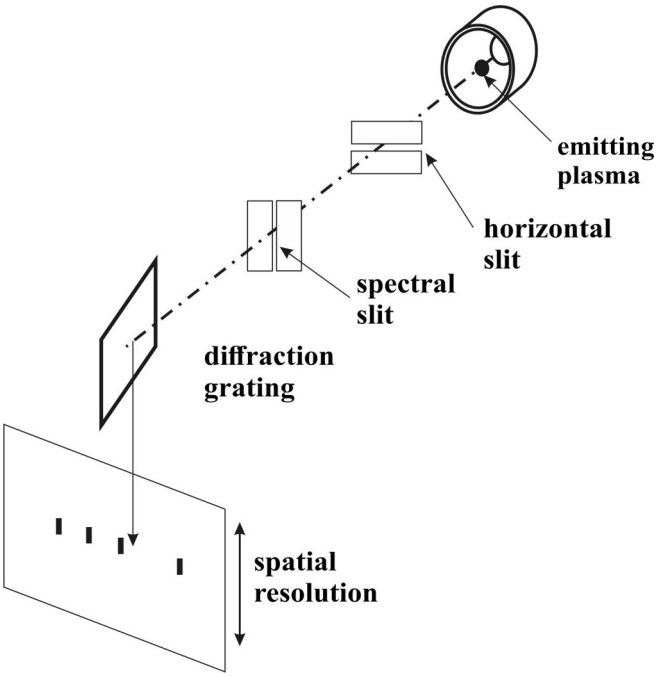


FIG. 3. The scheme of the grazing incidence spectrometer with spatial resolution.

of the resonance lines of Ar IX and Ar X (ionization potentials are $I_{\mathrm{Ar\,IX}} = 422.4\,\mathrm{eV}$ and $I_{\mathrm{Ar\,X}} = 478.7\,\mathrm{eV}$) indicates that the electron temperature of moving hot plasma is in the range 50–100 eV.

## IV. DISCUSSION OF THE ORIGIN OF 10.8-nm SPECTRAL LINE

It should be underlined that the appearance of the 10.8-nm line requires a precondition of the discharge cavity by several tens of discharges with Xe as a working gas at a pressure of about 100 Pa. The possibility of assigning of 10.8-nm line to transitions in Xe ions must be considered. The spectrum (a) from Fig. 5 together with a typical Xe spectrum of precondition discharge is given in Fig. 7. The line under consideration is on the short wavelength shoulder of the array

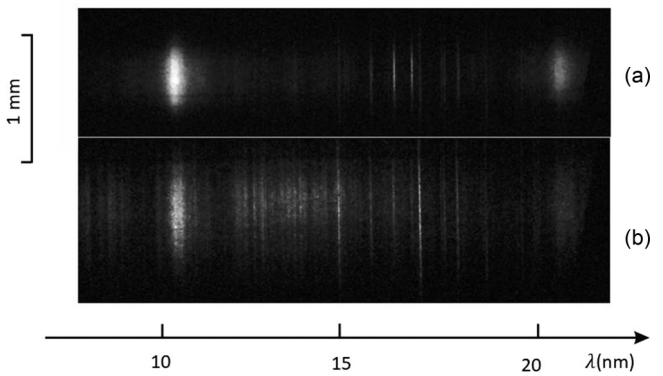


FIG. 4. Spatially resolved EUV spectra: (a) 40–60 ns, (b) 70-90 ns. Times are given with respect to the beginning of the discharge current. The scale in the direction of spatial resolution is given.

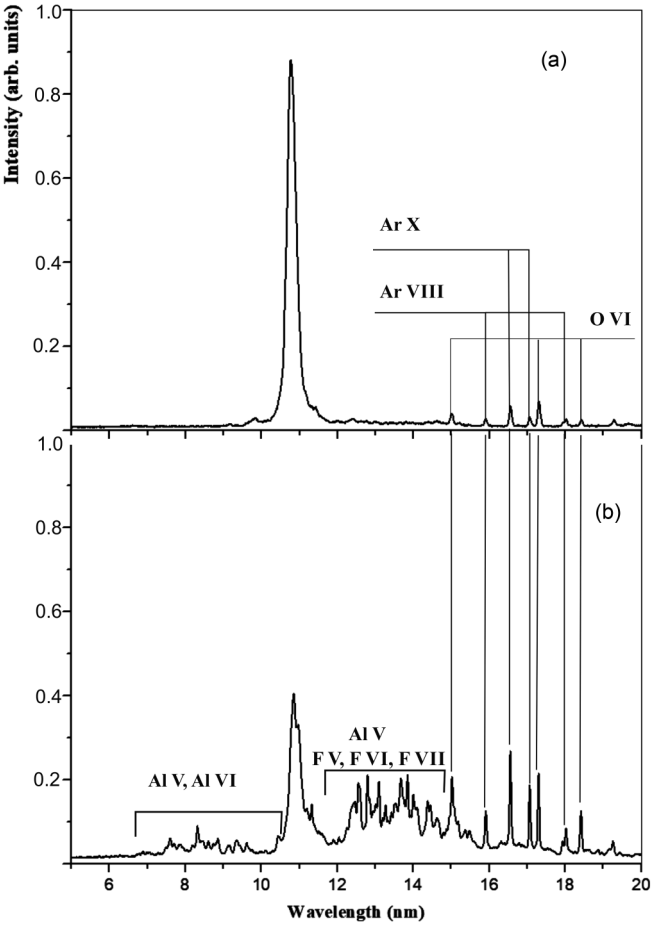


FIG. 5. The spectrograms of the spectra images Figs. 4(a) and 4(b).

of spectral lines in Xe XI [7]. No other spectral lines of Xe ions can be seen in the spectrum under study. In the normal regime the discharge cavity is filled with Ar, and it is not possible to get a 10.8-nm line with admixture of Xe to Ar

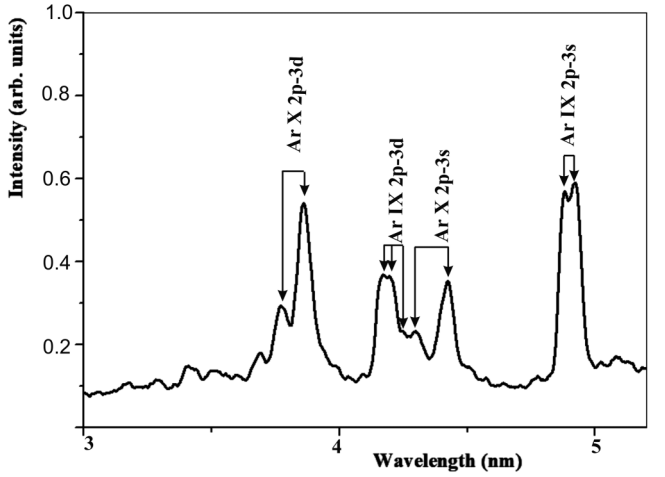


FIG. 6. The spectrum of resonance transitions of Ar IX and Ar X. The spectral profile does not change for frame times within 40–80 ns.

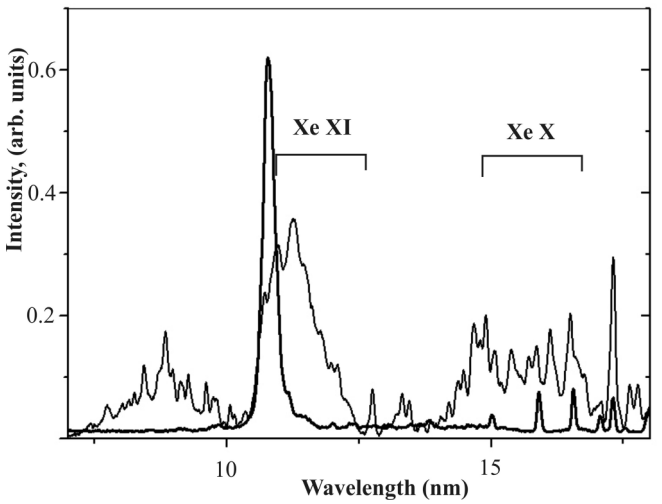


FIG. 7. The Xe spectrum together with spectrum in Fig. 5(a).

until the precondition with Xe filling is done. Anyhow, it is not feasible to propose a mechanism which would explain the selective population only of several levels in the electron configuration $4p^5 4d^9$ of Xe XI, resulting in an intensity of radiation more than total plasma radiation intensity in EUV. So, most likely the spectral line under consideration does not belong to transitions in Xe ions.

The spectral envelope of intense EUV radiation covers the region of Ry transitions $3p-nd$ and $3p-ns$ in Ar VIII; see Fig. 8(a). Its maximum corresponds to a $3p-9d$ transition, and its width more than five times exceeds the width of the apparatus profile of the spectrometer (discussed below). One of the state selective mechanisms of a level's population is charge exchange. At first glance it looks quite plausible in the present case. The spatial structure of the discharge plasma includes the hot core, which moves effectively along the axis of the discharge and cold working gas in front of the shock wave. These regions are in close contact, and multiply charged ions of hot plasma can effectively interact with neutral atoms of working gas. The problem is that the $9d$ level of Ar VIII is quite far from the resonance with the ground state of Ar I. A simple estimation, based on energy conservation, can be done. The sum of the ionization potential of Ar I (15.76 eV) and the potential energy of two charged particles with charges $+1e$ and $+7e$ on a distance of about $\sqrt{\sigma_{\text{ch.ex.}}}$ should be about the ionization energy of the $9d$ state in Ar VIII (11.08 eV [7]). Taking the value of the charge exchange cross section as $\sigma_{\text{ch.ex.}} \cong 10^{-14}$ cm$^2$, we get the potential energy of repulsion of about 10 eV. So, the above mentioned sum is 25.76 eV, that is considerably larger than 11.08 eV of the $9d$ state. The closest value to this level of Ar VIII is $6d$ (the ionization potential is 24.97 eV). This simple estimation matches to the classical over barrier model [8,9], which gives the most probable main quantum number of the attached electron for our case as $n = 5-6$. Actually the result of the charge exchange

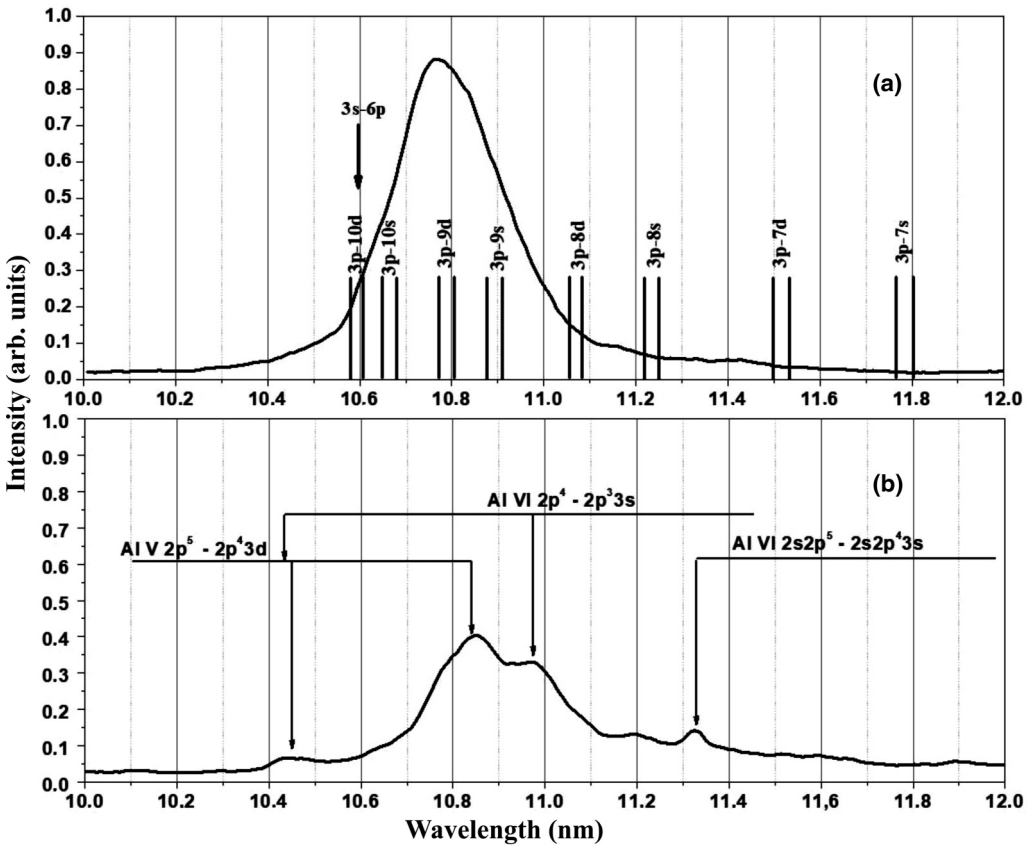


FIG. 8. Detailed spectral profile of EUV radiation of conical discharge in the range 10–12 nm. (a) 40–60 ns, the positions of Rydberg series of Ar VIII are shown. (b) 70–90 ns, the transition in Al V, Al VI are marked.

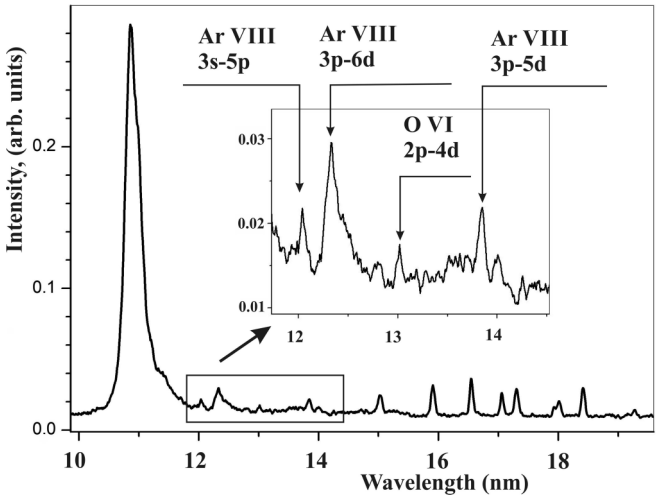


FIG. 9. An example of spectrum with enhanced intensity of Ar VIII $3p-6d$ transition.

to the $6d$ level of Ar VIII can be seen in the spectra; an example is given in Fig. 9. Here the intensity of the $3p$-$6d$ line is obviously more than $3p$-$5d$. But still it is much less than the intensity of the 10.8-nm line and it fluctuates considerably from discharge to discharge. A possible conclusion is that hot plasma in the point of the collapse of the conical shock wave does not immediately interact with cold working gas.

A detailed structure of the transient zone between hot plasma in the point of collapse of a conical shockwave and cold working gas in front of a shock wave can be obtained by means of numerical modeling of the plasma motion. But it is reasonable to propose that the ion composition of the system of hot plasma plus cold working gas changes along the discharge axis from Ar X–Ar IX (hot region) to Ar I (cold working gas) on the distance about the shock wave front width. So, the Ar I particle enters the hot plasma and before charge exchange with Ar IX undergoes interaction with hot electrons, which produce the ionization and excitation of Ar I. The cross sections of inelastic interaction of electrons (the energy in the range 50–100 eV, that corresponds to the electron temperature of plasma, containing ions Ar IX and Ar X) with Ar I are [10] excitation $\sigma_{ex} = 0.6 \times 10^{-16}$ cm$^2$ and ionization $\sigma_{ion} = 2.7 \times 10^{-16}$ cm$^2$. The upper limit of the electron concentration, estimated from the visible plasma compression (ratio of the diameter of rear aperture of discharge cavity and the transverse size of hot plasma), is $n_e \sim 10^{18}$ cm$^{-3}$. So, the value $(\sigma v_{el} n_e)^{-1} \geqslant 10^{-10}$ s. Taking into account that electron density gradually changes from about zero value in the cold region, the above estimation can be up to nanosecond scale. This shows that in the nanosecond time scale part of the Ar I atoms will be ionized and another part will be excited. That makes possible the charge exchange of highly ionized argon with excited neutral atoms. For the concentration of Ar I $n_{Ar\ I} \cong 2 \times 10^{16}$ cm$^{-3}$, velocity of Ar IX $v_{Ar\ IX} \cong 2 \times 10^6$ cm/s (corresponds to the energy 100 eV), and charge exchange cross section $\sigma_{ch.ex.} \cong 10^{-14}$ cm$^2$, we get $(n_{Ar\ I} v_{Ar\ IX} \sigma_{ch.ex.})^{-1} \cong 2.5 \times 10^{-9}$ s. Radiation times of Ar I for resonance transitions $3p$-$4s$, $3p$-$4d$ are in the range of 1–10 ns [7], the radiation times of $4s$-$4p$ transitions are even in the range of hundreds of ns, so there is enough time for excited Ar I to take part in charge exchange. The displacement of hot plasma on the value about 0.01 cm during 1 ns (effective velocity is about $10^7$ cm/s) will supply a new portion of Ar I atoms into the interaction zone instead of "burned."

The role of precondition discharges can be the removing from the inner surface of the discharge cavity the absorbed water, nitrogen, and oxygen that can influence upon the structure of the front of a conical shock wave. Heavy Xe ions can do that much more effectively than Ar ions. Comparison of the detailed spectra in Figs. 8(a) and 8(b) shows that at 70–90 ns from the beginning of the discharge the intensity of 10.8-nm line goes down and the lines of ions of Al, eroded from the inner wall of $Al_2O_3$ discharge cavity, appear. The discharge current at this moment does not reach its maximum, which takes place at 200 ns, and the hot compact plasma still can be seen (Fig. 2), but the line at 10.8 nm disappears. It can be connected with the change of the composition of the plasma in the transient zone by eroded material and diminishing the percentage of Ar I, necessary for charge exchange.

## V. WIDTH OF 10.8-nm LINE

Full width at half maximum of the 10.8-nm spectral line is 0.3 nm (see Fig. 8), that is about five times larger than the spectral resolution of the spectrometer. The visible size of the radiation source is less than 0.5 mm (see Fig. 3), so the working size of the grating for the 10.8-nm line is not larger than for other spectral lines. For that reason no additional apparatus broadening in comparison with other spectral lines can take place. Would the spectral profile of the 10.8-nm line contain only the lines of *nd* or *ns* Rydberg series of Ar VIII, they should be resolved. Two times increase of the spectral resolution in comparison with previous work [4] did not reveal any distinct spectral features.

The visible width of the 10.8-nm line cannot be of Doppler nature; in this case typical velocities of the emittig ions should be unrealistically high ($v > 10^8$ cm/s). The possible influence of Stark broaderning can be estimated, taking as above the upper limit of electron density $10^{18}$ cm$^{-3}$ and the electron temperature around 50–100 eV (the temperature corresponds to visible abundances of Ar ions in the plasma). Would the visible width be due to collisional broaderning, it will correspond to an unrealistically high collisional cross section about $10^{-12}$ cm$^2$. Taking mean Holtzmark field [11] for the estimation of input of quasistatic ion broadening we should also take into account that Rydberg levels of Ar ions under consideration are well splitted by the orbital moment and their shift is quadratic with respect to perturbing electrical field. The state $9d$ of Ar VIII interacts mostly with the state $9f$ (the energy splitting is 0.22 eV [7]). The estimation of the mean energy shift of $9d$ level gives the value about 0.01 eV (the oscillator strenghth is taken as 1). So, Stark broadening most likely is not responsible for the visible linewidth.

Analogous phenomena were found in experiments with laser produced plasma, expanding in gas media [12]. The main effect here is charge exchange of nitrogen nuclei and neutral nitrogen. The spectral lines of Rydberg series

$1s$-$nl(n = 5, 6, 7)$ were obtained in the wavelength region 1.9–1.94 nm and they are unusually broad ($\lambda/\delta\lambda \cong 200$). The visible spectral width is attributed to overlapping of many spectral lines in arrays $1'l' - n'l'nl$. Two electron charge exchange was proposed as the mechanism of the population of $n'l'nl$ states. In principle the same phenomenon can take place also in the present work. Taking into account that mentioned array of dielectronic satellites normally is on the long wavelength side of the parent line $1s$-$nl$ [13], in our case the parent line for the visible array at 10.8 nm could be transition $3s$-$6p$ in Ar VIII [see Fig. 8(a)]. Still some features are not consistent with the mentioned mechanism. The overall spectral profile in this case should look like an asymmetric long wavelength wing of parent line and contain structure, connected with spectral distribution of separate lines in the array. Actually we can see the increase of the intensity of the long wavelength wing of the Ar VIII $3p-6d$ transition in Fig. 9, which can be attributed to a dielectronic satellites array. But the problem of the visible spectral width of the 10.8-nm line is still open. The experiments with the usage of a spectrometer with higher resolution and theoretical analysis of plasma conditions in the transient zone can help to make a definite conclusion about the origin of the spectral width of the radiation under study.

## VI. CONCLUSION

The present work presents the physical picture of phenomena, taking place in fast conical discharge with Ar 80 Pa as the working gas. The collapse of a convergent conical shock wave gives rise to hot compact plasma (electron temperature 50–100 eV and size scale about 1 mm), which effectively moves with velocity about $10^7$ cm/s along the discharge axis during 80–100 ns. First at 40–50 ns this plasma emits the narrow band radiation at 10.8 nm (spectral width is 0.3 nm); this wavelength corresponds to a $3p$-$9d$ transition in Ar VIII. The intensity of the radiation exceeds the total plasma radiation in the EUV spectral band. When the material eroded from the inner wall of alumina conical discharge cavity reaches the hot plasma region, the 10.8-nm line disappears. The discharge cavity needs preconditioning by several tens of discharges with Xe as the working gas. The possible origin of the detected radiation can be charge exchange of Ar IX ions and excited atoms Ar I of the working gas. The problem of the origin of the visible spectral width of the detected radiation is still open. A definite conclusion about the origin and properties of EUV radiation in fast conical discharge needs the numerical modeling of the discharge plasma. The understanding of the main physical properties of discharge plasma is important for its possible practical applications as an EUV radiation source. Having produced more than $10^3$ discharges, we can foresee here also the technical problem of the ceramic cell erosion. The need of preconditioning by discharges with Xe limits the stable operation within several tens of discharges now. A possible technical solution implies the usage of an optimal current driver, which should produce the current pulse to the load with time length of several hundreds of nanoseconds, instead of several microseconds.

## ACKNOWLEDGMENT

The work was done according the working plans of the Institute of Spectroscopy of Russian Academy of Sciences.

[1] C. D. Macchietto, B. R. Benware, and J. J. Rocca, Opt. Lett. **24**, 1115 (1999).
[2] N. A. Bobrova, S. V. Bulanov, T. L. Rasinkova, and P. V. Sasorov, Plasma Phys. Rep. **22**, 349 (1996).
[3] P. S. Antsiferov and L. A. Dorokhin, Phys. Plasmas **21**, 042119 (2014).
[4] P. S. Antsiferov, L. A. Dorokhin, and K. N. Koshelev, J. Phys. D: Appl. Phys. **51**, 165601 (2018).
[5] P. S. Antsiferov, L. A. Dorokhin, Yu. V. Sidelnikov, and K. N. Koshelev, J. Appl. Phys. **105**, 103305 (2009).
[6] P. S. Antsiferov, L. A. Dorokhin, and P. V. Krainov, Rev. Sci. Instrum. **87**, 053106 (2016).
[7] A. Kramida, Yu. Ralchenko, J. Reader, and NIST ASD Team, *NIST Atomic Spectra Database, version 5.1* (National Institute of Standards and Technology, Gaithersburg, MD, 2018), http://physics.nist.gov/asd.
[8] R. Mann, F. Folkmann, and H. F. Beyer, J. Phys. B: At. Mol. Phys. **14**, 1161 (1981).
[9] A. Barany, G. Astner, H. Cederquist, H. Danared, S. Huldt, P. Hvelplund, A. Johnson, H. Knudsen, L. Liljeby, and K.-G. Rensfelt, Nucl. Instrum. Methods Res. B **9**, 397 (1985).
[10] A. Zecca, G. P. Karwasz, and R. S. Brusa, Riv. Nuovo Cimento **19**, 35 (1996).
[11] H. R. Griem, *Spectral Line Broadening by Plasmas* (Academic Press, New York, 1974).
[12] F. B. Rosmej, A. Ya. Faenov, T. A. Pikuz, A. I. Magunov, I. Yu. Skobelev, T. Auguste, P. D'Oliveira, S. Hulin, P. Monot, N. E. Andreevk, M. V. Chegotovkand, and M. E. Veismank, J. Phys. B: At. Mol. Opt. Phys. **32**, L107 (1999).
[13] K. N. Koshelev, J. Phys. B: At. Mol. Opt. Phys. **21**, L593 (1988).